Application of MODTRAN™ to Extra-Terrestrial Planetary Atmospheres

Lawrence S. Bernstein, Alexander Berk, and Robert L. Sundberg
Spectral Sciences, Inc., Burlington, MA

ABSTRACT

MODTRAN™ [1] is a widely used radiative-transfer (RT) code for computing the transmission and emission of the Earth's atmosphere. However, the RT algorithms used in MODTRAN™ are generally applicable to any layered atmosphere, and, in principle, can be applied to any planetary atmosphere. The primary modification required for this application is the development of the appropriate spectral properties data bases for the particular species associated with a given planetary atmosphere. We demonstrate the application of a modified MODTRAN™ to Neptune for which the primary absorbing atmospheric species are H_2, CH_4, C_2H_6, and C_2H_2. For the carbon-containing species, we have developed molecular band model parameters, and for H_2 we have utilized continuum parameters computed by others. Additionally, we have incorporated models to account for the CH_4 and C_2H_6 clouds and hazes which form in the extremely cold upper atmosphere of Neptune. We present calculations both for the solar reflective spectral region, ~0.4-2 μm, as well as the thermal IR emission region, ~3-20 μm. Comparisons are made with archival data over the visible-long wavelength IR wavelength regime.

1. INTRODUCTION

The need for rapid and accurate predictions of planetary spectra over a broad wavelength regime is increasing at a fast pace. This is primarily fueled by the discovery of some ~250 extrasolar planets to date, as well as continued interest in our own planetary system. There are a number of widely used radiative transfer (RT) computer models [1-11] that are routinely used to predict planetary spectra. However, they are generally specialized to a constrained wavelength regime or a particular spectral signature and often are not readily useable by non-experts in RT. We explore here the potential for applying MODTRAN™, a widely used terrestrial RT code, to many types of planetary RT problems over a very broad wavelength regime.

We describe the modifications made to the code and demonstrate its application through comparison to observational data for Neptune covering the 0.4-200 μm spectral range. Fig. 1. highlights the nature of the challenge by comparing planetary spectra for Earth and Neptune. Neptune's radiance is much lower than Earth's because it is much colder, ~60 K vs. ~300 K, and much further away from the sun, ~4.5×10^9 km vs. ~1.5×10^8 km. Of more interest are the large differences in the detailed spectral structure. The primary emission-absorption features for Earth are due to H_2O and CO_2. In contrast, on Neptune they are due to CH_4 and H_2. The central issue in generalizing MODTRAN™ for planetary applications is the incorporation of new spectral data bases for the much wider variety of molecular species, clouds, and aerosols encountered on other planets and moons.

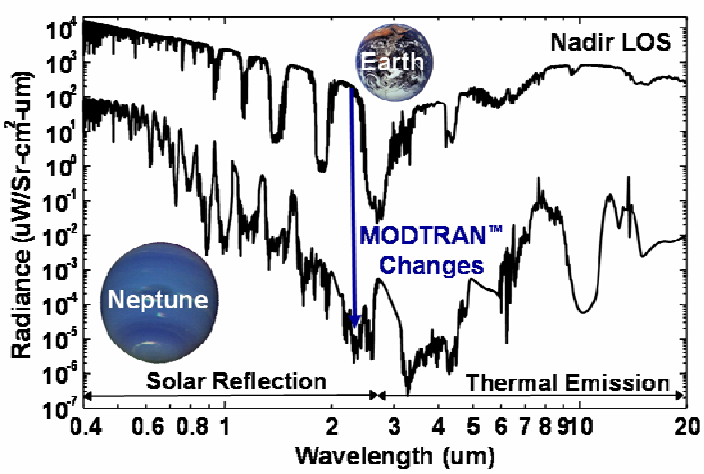

Fig. 1. Examples of modified MODTRAN™ calculations of the remotely view spectral signatures of the Earth and Neptune for a nadir line of sight.

2. MODTRAN™ OVERVIEW

MODTRAN™ is the product of a long standing and continuing collaboration, starting in 1987, between Spectral Sciences, Inc. and the Air Force Research Laboratory. The exact number of regular users is not well established, but conservative estimates place it at well over 2,000. The code is well validated and a yearly technical conference is held to discuss problems, progress, and applications. It's key attributes are summarized below:

- 1D Atmospheric Radiative Transfer Model
- IR / Vis / UV Transmittances, Radiances and Fluxes
  - 1-50,000 cm^{-1} or 0.2-10^4 μm
- Band model and k-distribution RT approaches
- 0.1, 1.0, 5.0 & 15.0 cm^{-1} resolution molecular band models
  - Based on HITRAN line parameter data base [12]
- Stratified Molecular / Aerosol / Cloud Atmosphere
  - Standard and User-Specified data bases
- Solar and Thermal Scattering
  - 2-Stream and DISORT N-Stream
- Spherical Refractive Geometry
- Surface emission & reflectance with BRDF
- Assumes LTE (Local Thermodynamic Equilibrium)

Because of the LTE assumption, MODTRAN™ will work best for problems in which the observational line of sight (LOS) probes atmospheric regions of sufficient pressure to validate this assumption. While different species/spectral bands go out of LTE at different pressures, generally speaking, LTE is a reasonable assumption for pressures exceeding ~1 mbar. Calculations can be performed at a variety of spectral resolutions, which enables one to optimize computational time for a particular problem.

There are two types of RT approaches within the code, which are depicted in Fig. 2. MODTRAN™ uses molecular band models to efficiently and fairly accurately compute the transmittance for a *finite spectral interval* using analytical approximates. In contrast, line by line (LBL) codes, while slightly more accurate, break a spectral interval into thousands of spectral points, each requiring separate evaluation. Generally, a band model approach affords about a two orders of magnitude speed advantage over a LBL approach. The band model is based on a statistical description of each spectral interval, embodied in band model parameters, which include an effective number of lines, an average integrated line strength, and the Lorentz (pressure broadening) and Doppler (velocity broadening) line widths which determine the line shape. The band model parameters can be determined either from experimental measurement of species transmittances or more typically from line parameter compilations, such as HITRAN, [12] assuming that the lines for a particular species/band are available.

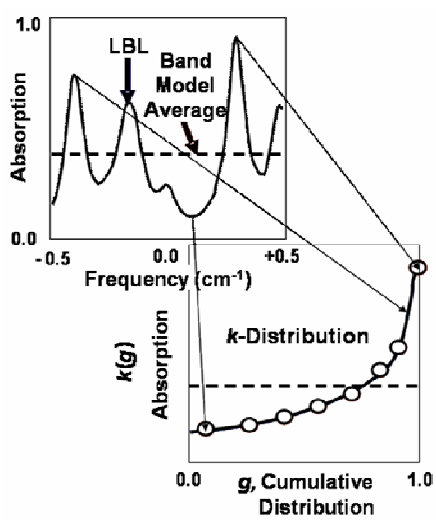

Fig. 2. Overview of the band model and k-distribution radiative transfer approaches used in MODTRAN™.

The band model approach works best for problems which only involve molecular absorption and emission. The methods for solving the coupled molecular absorption-emission and scattering problem require that the LOS transmittance can be expressed by a Beer's law formulation (i.e., transmittance = exp(-optical depth)). The fast analytical approximations used for band models do not obey Beer's law, hence a different RT approach is required. In this case, the k-distribution approach is applied. In this method, a finite spectral interval is represented in terms of just a handful of absorption coefficients (of order 20), as opposed to thousands for a LBL approach. Each of these is treated in a Beer's law fashion with the resulting transmittance weighted by the frequency of occurrence of the particular k-value in the spectral interval. This method takes advantage of the fact that there is a high degeneracy among absorption coefficient values in an interval. MODTRAN™ employs a pre-computed table of k-distributions that are directly tied to the band model parameters, and can be extracted on the fly, allowing for excellent computational efficiency, even for scattering problems. Band model approaches can also be problematic for atmospheres with large species concentration and temperature gradients; however, the k-distribution method usually works well in these situations. Fig. 3. shows an example validation comparison which is typical of the kind of accuracy obtained when comparing to well characterized field data and the more rigorous LBL approach.

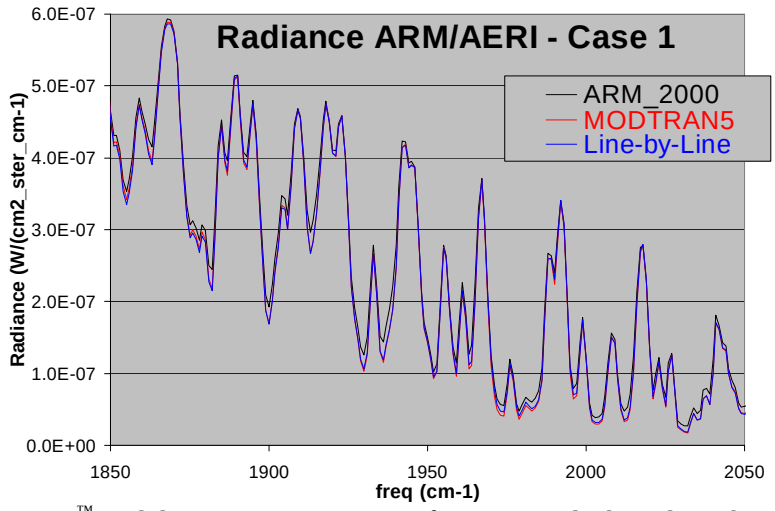

Fig. 3. Example MODTRAN™5 validation against AERI interferometer up-looking data taken at the DOE ARM site and FASE line by line predictions.

3. CODE MODIFICATIONS

The primary changes to the code involved adding a variety of different spectral data bases appropriate to the species encountered in Neptune's atmosphere as well as the other outer planets and moons (e.g., Saturn, Uranus, Jupiter, and Titan). The specific modifications are summarized below:

- Band model parameters
  - Profile species currently included
    - CH_4, C_2H_6, C_2H_2, HCN, CO, H_2O
  - Extended temperature range down to 30K
  - CH_4 far from complete
    - Patchwork of theory, lab and field data [12-14]
- Continuum parameters
  - Added Rayleigh cross sections for H_2, He, & CH_4 [15]
  - Extended line tails to higher pressures
    - Including non-Lorentz behavior of far tails [14]
  - Added H_2-H_2 and H_2-He collision-induced continua [16]
- Cloud and aerosol parameters
  - Added three Neptune cloud/haze layers [17, 18]
- Scaled solar illumination spectrum for different sun-planet distance

Methane is the dominant molecular absorber, however its spectroscopy over the entire wavelength regime of interest is still incomplete and not known at the desired level of accuracy for many applications. The ultimate goal is to obtain a complete and accurate line compilation. However, this is a daunting goal as methane has an enormous number of lines, particularly at moderate to high temperatures. It is only recently that really complete line compilations for H_2O have been developed, a molecule with three as opposed to nine vibrational degrees of freedom for CH_4. While quite useful, the HITRAN CH_4 data base contains many unassigned lines and stops short of 1 μm. A laboratory-derived lower resolution band model data base has been developed specifically for planetary applications [19]. However, it does not extrapolate well into conditions too different from the laboratory conditions from which it was derived and it is limited to 10 cm^{-1} spectral resolution. The situation below 1 μm is even more approximate, where a set of temperature-independent absorption coefficients has been derived directly from observations of the outer planets [13]. A comparison of these different sources of CH_4 absorption coefficients is presented in Fig. 4. It is seen that the HITRAN data base is missing bands in trough regions between the stronger features. It is seen that the laboratory-derived absorption coefficients do not properly reproduce the absorption levels for the two strongest bands they have in common with HITRAN. This is due to the fitting method used in their derivation; it properly reproduces the laboratory data but it leads to unphysical parameter values.

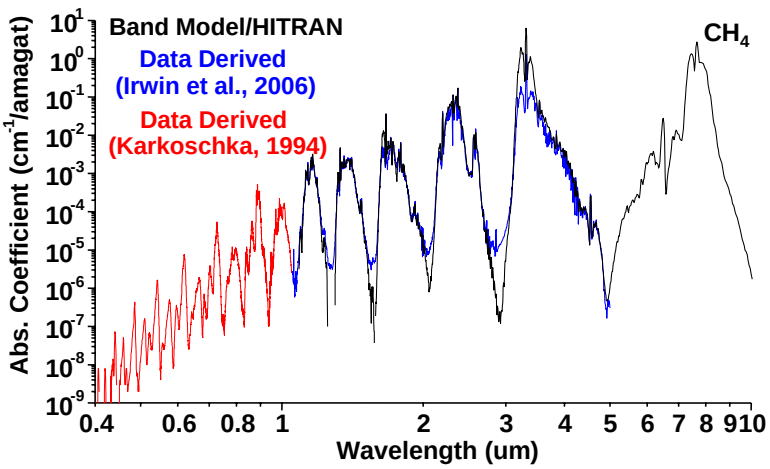

Fig. 4. Comparison of room temperature CH_4 absorption coefficients derived from a variety of approaches.

The collision induced absorption due to H_2-H_2 and H_2-He collisions also plays a dominant role in the RT of Neptune and the other outer planetary bodies. This is due both to the high abundances of H_2 and He (85% and 15% for Neptune) and more importantly to the high pressures on these bodies. The Collision Induced Absorption (CIA) is proportional to the square of the pressure, which becomes quite large as one descends into these atmospheres. An example of the enormous spectral extent spanned by the CIA effect is shown in Fig. 5.

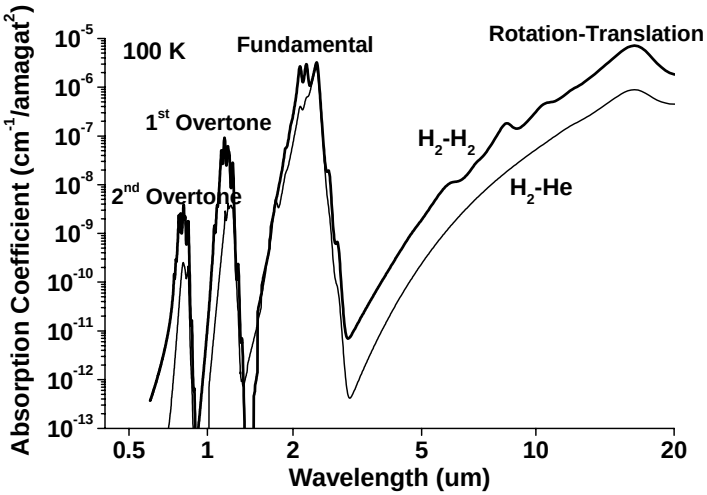

Fig. 5. Examples of the collision induce absorption coefficients at 100 K for H_2-H_2 and H_2-He collisions.

Hazes and clouds are common occurrences for the outer planets due to the extremely cold temperatures and moderate pressures encountered in the tropopause and lower stratosphere. Hydrocarbon species, such as CH_4 and C_2H_6, readily condense under these conditions. MODTRAN™ models arbitrary aerosol haze profiles with multiple haze species as well as multiple cloud layers. The issue is providing the scattering and absorption optical properties for the haze and cloud particles. In the case of Neptune, there are three identified cloud/haze layers for which approximate optical properties have been estimated. The optically thin stratospheric haze contains condense hydrocarbons, primarily ethane. For this layer, the sum of the equatorial region stratospheric spectral optical depth (τ_λ) curves from Fig. 14 of [17] was fit to the Angstrom Law giving $\tau_\lambda = 0.008 / \lambda^{3/4}$ (wavelength λ in microns). The condensed methane upper troposphere cloud was given a constant optical depth of 0.087, again based on Fig. 14 of [17]. For both of these upper clouds, a scattering albedo of 1 was assumed. The optically thick lower tropospheric cloud, with cloud top near ~3.5bar, was modeled with a spectrally constant optical depth of 10 and scattering albedos of 0.23 at 1.27 μm and 0.18 at 1.56 μm [18]. For all three cloud/haze levels, the double Henyey-Greenstein phase function ($g_1 = 0.90$, $g_2 = -0.11$, $f_1 = 0.42$) of [20] was assumed. Fig. 6 illustrates the spectral extinction curves used in our analysis.

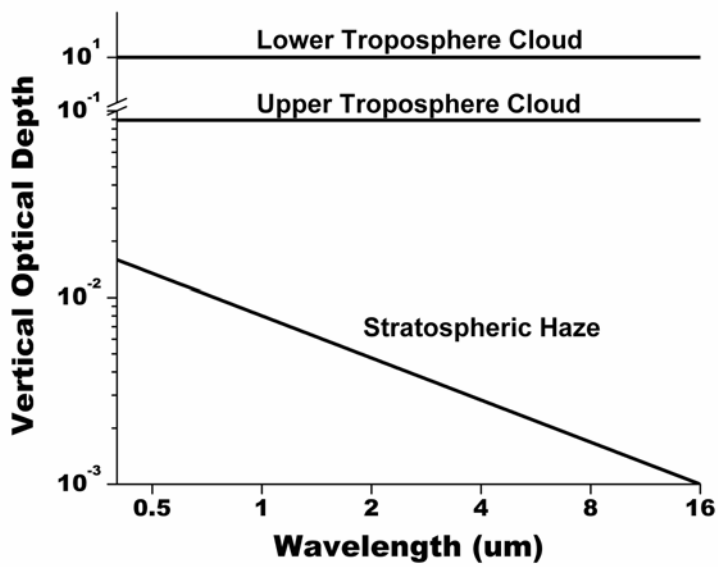

Fig. 6. Neptune's equatorial region cloud/haze spectral opacities.

4. APPLICATION TO NEPTUNE

We have performed a number of comparisons between MODTRAN™ modified for planetary applications and observational data for Neptune over a broad wavelength region, spanning the visible through far infrared spectral domains. These calculations are based on the reference atmosphere temperature and species concentration profiles depicted in Fig. 7 [21-23]. Before discussing the comparisons, it is helpful to first consider the individual spectral contributions to a vertical LOS transmission spectrum as shown in Fig. 8. The dominant role of CH_4 is clearly evident, where it is seen that CH_4 alone prevents one from viewing deeper than about 10 bar over the ~2-10 μm region. Similarly, the H_2 CIA features prevent seeing deeper than ~1 bar beyond 10 μm. One can probe deeper into the atmosphere in the visible and near infrared regions, where even at 10 bar some light can still penetrate. Approximately 30 bar is the deepest that one can peer into Neptune's atmosphere. The absorptions due to the trace species, C_2H_6, C_2H_2, and CO are much weaker and these species are most readily observed in the stratosphere, below ~10 mbar, where they aren't completely obscured by stronger CH_4 and H_2 absorptions.

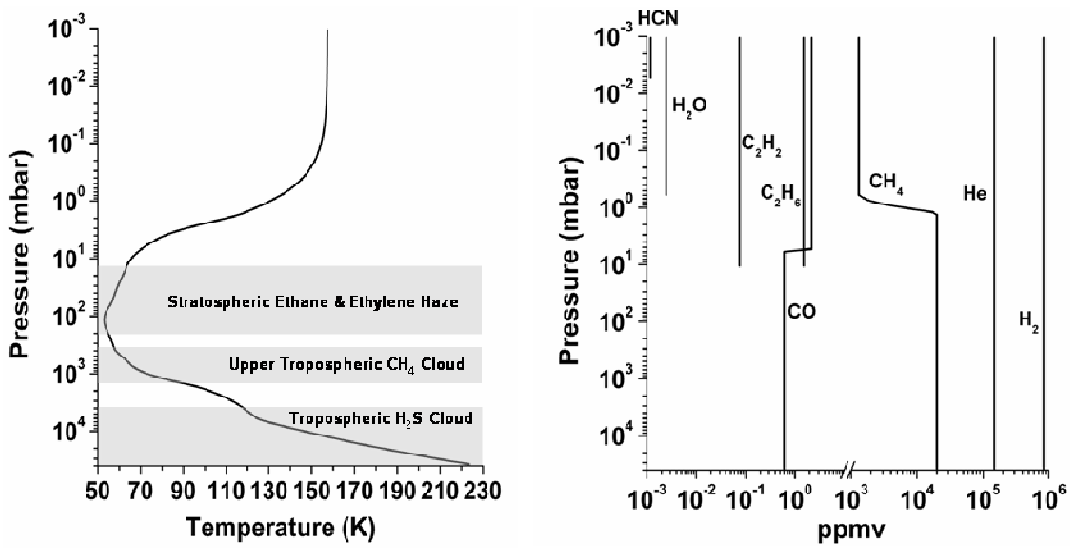

Fig. 7. Temperature and species concentration profiles for Neptune. The approximate pressure-altitude ranges for the previously retrieved haze and cloud layers are also indicated.

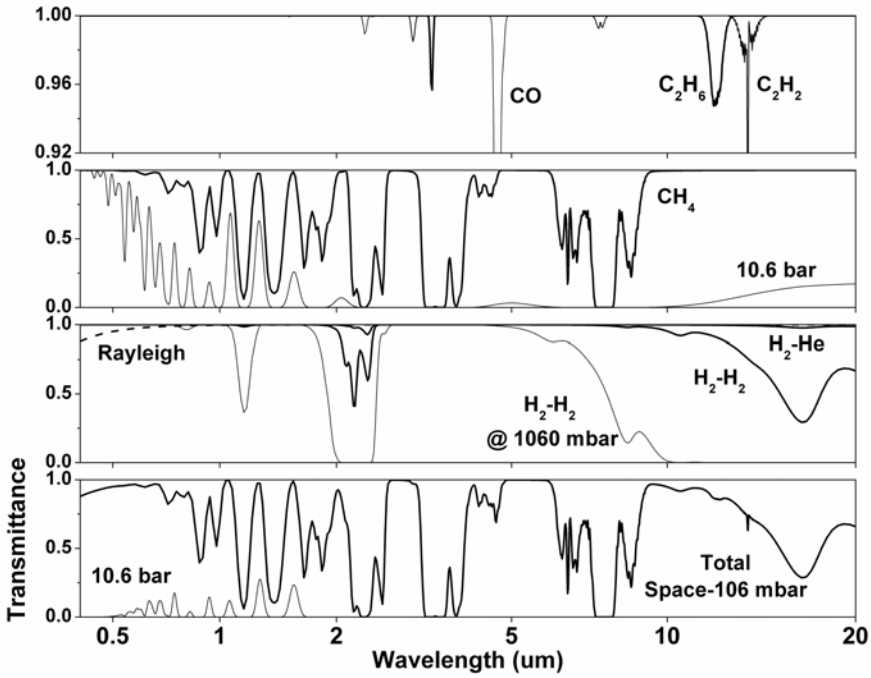

Fig. 8. Species spectral transmission components for a nadir path from Space to 106 mbar. The top panel shows CO, C_2H_6, and C_2H_2. The panel below that shows CH_4 only (thick line). The next panel down illustrates H_2-He and H_2-H_2, (thick lines) as well as Rayleigh scattering (dashed line). The bottom panel shows the total for the three panels above (thick line). Also shown are the effects of higher pressure (thin lines) on the total, the H_2-H_2 collision induced absorption, and the CH_4 transmission components.

A comparison for the long wavelength IR spectral region, ~17-200 μm (50-600 cm^{-1}), is shown in Fig. 9. This is an H_2 dominated region. It is seen that a slight increase in the reference profile temperature is required to give a reasonable match to the data [21, 24, 25]. As noted by Burgdorf et al. [21], one can obtain a nearly perfect fit to the data by adding both a constant temperature to the profile and adjusting the profile temperature gradient slightly in the lower stratosphere region. Our goal here, and in the other comparisons, is not to adjust all available parameters to achieve an ultimate fit to the data, but rather to demonstrate that the modified MODTRAN™ can produce good results across a very broad wavelength regime.

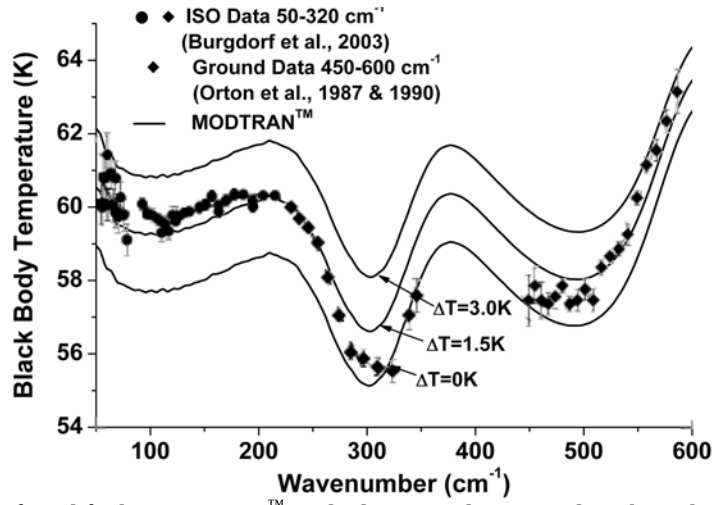

Fig. 9. Comparison of modified MODTRAN™5 calculations to long wavelength IR data for Neptune. The calculations are based on the reference temperature and species profiles shown in Fig. 7.

The next two fits focus on mid-IR data at low and high spectral resolution, Figs. 10 and 11, respectively. Fig. 10 features the entire 12 μm C_2H_6 band as well as pieces of the 13.7 μm C_2H_2 band and the 7.8 μm CH_4 band [26]. The effect of atmospheric transmission on the CH_4 band is clearly seen. We assumed (just a guess) that the observation elevation angle was 60 deg, which slightly over estimates the effect of atmospheric transmittance on the methane band. Because of the perfect spectral correlation between terrestrial methane absorption lines and the Neptune methane emission lines, one cannot employ the standard astronomy observational method of using a nearby star to estimate the absorption due to the Earth's atmosphere. The standard method only determines an effective average for a finite spectral interval, much broader than the width of a methane line. The high spectral resolution data comparison [27] in Fig. 11, while reasonable, highlights some of the problems with the C_2H_6 HITRAN data base. Close inspection reveals that there is missing intensity in a number of locations. This is due to the fact that the lines for an important ethane hot band are not included in HITRAN. Also, the peak intensities in the two longest wavelength lines are much too high. Again this may be attributed to inaccuracies in the HITRAN data base. Blass has developed an improved ethane line compilation that addressed these deficiencies and were validated in earlier analysis [28]. The over prediction for the ~12.09 μm feature is likely due to an atmospheric transmission loss that was not included in these calculations.

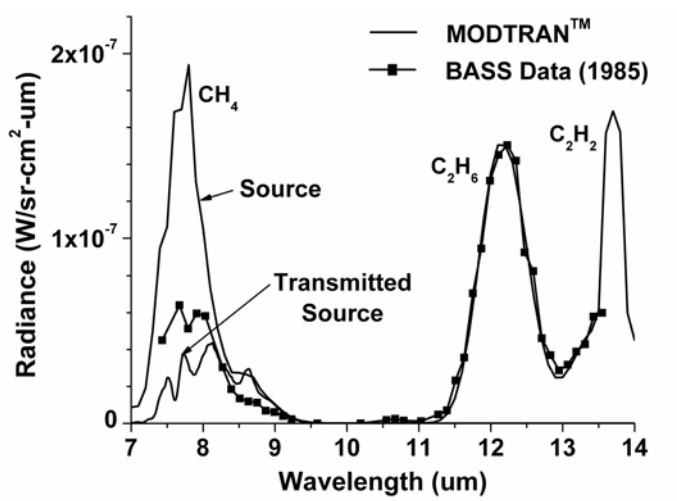

Fig. 10. Comparison of modified MODTRAN™5 calculations to low spectral resolution mid-wavelength IR data for Neptune. The calculations are based on the temperature and species profiles shown in Fig. 7, where a +3K altitude-independent temperature increase was required to fit the 12 μm C_2H_6 feature. The dramatic effect on terrestrial atmospheric transmission on the 8 μm CH_4 band for the Mauna Kea observing site is also indicated.

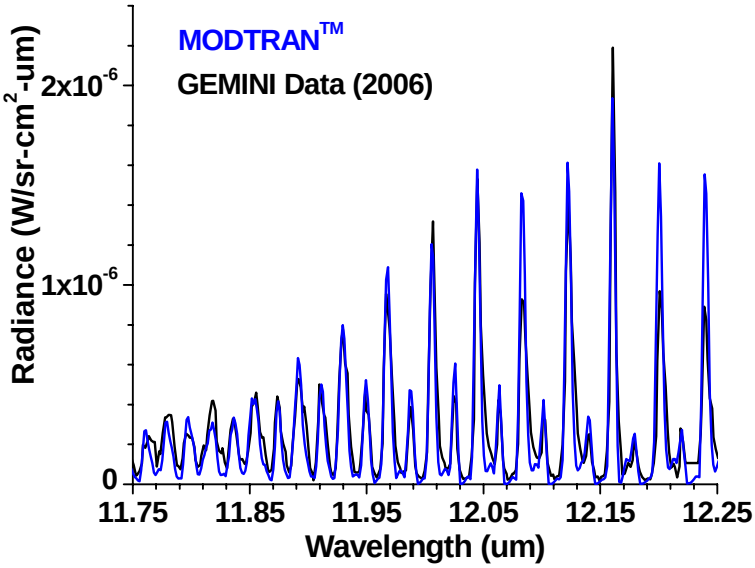

Fig. 11. Comparison of modified MODTRAN™5 calculations to high spectral resolution data for the 12 μm C_2H_6 band for Neptune. The temperature profile was increased by +10K for these calculations.

The final comparison [13, 29] covers the visible-near infrared spectral region and is shown in Fig. 12. Below ~1.5 μm the geometric albedo is almost entirely due to Rayleigh scattering with the absorption features due to CH_4. At longer wavelengths, the influence of the scattering from a low lying stratospheric haze layer is evident. The haze was modeled as a ~2% reflection at 1 μm with a 1/λ wavelength dependence. A transmission loss corresponding to an effective haze layer pressure altitude of ~25 mbar was included.

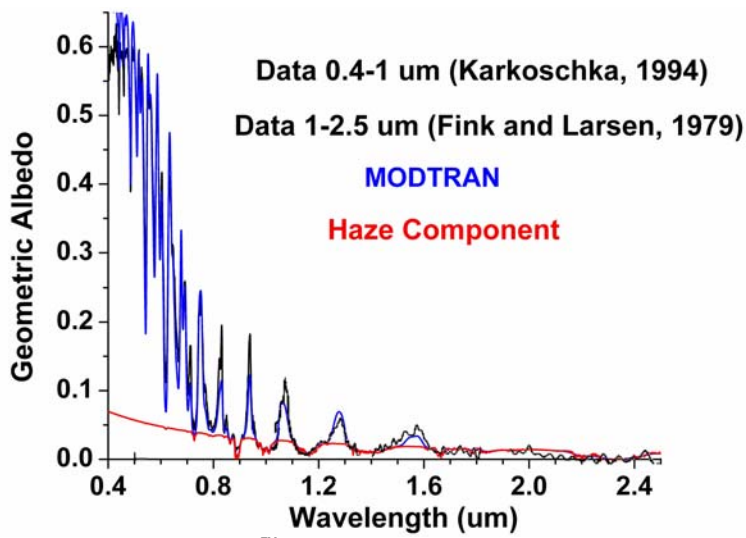

Fig. 12. Comparison of modified MODTRAN™5 calculations to observations of Neptune's geometric albedo over the visible-near IR wavelength region. Also shown is the estimated contribution of a high altitude optically thin scattering haze layer to the albedo.

5. CONCLUSIONS AND FUTURE EFFORTS

The primary conclusions include:

- We have developed a prototype of MODTRAN™5 modified for application to planetary atmospheres.
- The initial data comparisons for Neptune appear reasonable over a very broad wavelength regime.

Future efforts include:

- Adding more species and extend to higher temperature
- Improving the CH_4 spectral data base
- Including new cloud and haze models
- Adding generalized stellar source and geometry models
- Validating against other codes and more data (e.g., Saturn, Jupiter, Titan,…)
- We anticipate development and testing of the initial prototype to be completed in early 2008.

6. ACKNOWLEDGEMENTS

The authors express their gratitude to H. B. Hammel (Space Science Institute), M. Sitko (Space Science Institute), and the Gemini Observatory for providing the high resolution Neptune ethane spectrum, to D. Lynch (The Aerospace Corporation) and R. Russell (The Aerospace Corporation) for providing the BASS data, to T. Hewagama (NASA Goddard SFC) for technical discussions, to G. Anderson (Air Force Research Laboratory) for providing the MODTRAN™ validation calculation, to A. Jorgensen (Michigan Technological University) for assistance with the collision induced data bases, to P. Irwin (University of Oxford) for technical discussions, to B. Hesman (National Radio Astronomy Observatory) for providing the Neptune atmospheric profiles, to J. Duff (Spectral Sciences, Inc.) for computing Mie cloud/haze parameters, and to Spectral Sciences, Inc. for funding this IR&D activity.

7. REFERENCES

1. Berk, A., Anderson, G.P., Acharya, P.K., Bernstein, L.S., Muratov, L., Lee, J., Fox, M., Adler-Golden, S.M., Chetwynd, J.H., Hoke, M.L., Lockwood, R.B., Gardner, J.A., Cooley, T.W., Borel, C.C., Lewis, P.E., and Shettle, E.P., MODTRAN5: 2006 Update, Proc. SPIE, Vol. 6233, 62331F, 2006.
2. Bailey, J., VSTAR – A New High-Spectral-Resolution Atmospheric Radiative Transfer Code for Mars and Other Planets, Proc. 2nd International Workshop on Mars Atmosphere Modelling and Observations, F. Forget, *et al*., 148, 2006.
3. Buehler, S.A., Eriksson, P., Kuhn, T., von Engeln, A., and Verdes, C., ARTS, the Atmospheric Radiative Transfer Simulator, J. Quant. Spectrosc. Radiat. Transfer, Vol. 91, 65-93, 2005.
4. Clough, S.A., Shephard, M.W., Mlawer, E.J., Delamere, J.S., Iacono, M.J., Cady-Pereira, K., Boukabara, S., and Brown, P.D., Atmospheric Radiative Transfer Modeling: A Summary of the AER Codes, Short Communication, J. Quant. Spectrosc. Radiat. Transfer, Vol. 91, 233-244, 2005.
5. Dothe, H., Duff, J.W., Gruninger, J.H., Acharya, P.K., and Berk, A., SAMM2, SHARC-4 and MODTRAN4 Merged (User's Manual), Environmental Research Paper No. 1260, 2005.
6. Edwards, D.P., GENLN2: A General Line-By-Line Atmospheric Transmittance and Radiance Model, Tech. Rep. NCAR/TN-367+STR, 1-147, 1992.
7. Kunde, V.G. and Maguire, J.C., Direct Integration Transmittance Model, J. Quant. Spectrosc. Radiat. Transfer, Vol. 14, 803-817, 1974.
8. Lyapustin, A.I., Radiative Transfer Code SHARM for Atmospheric and Terrestrial Applications, Appl. Opt., Vol. 44, 7764-7772, 2005.
9. Meadows, V.S., and Crisp, D., Ground-Based Near-Infrared Observations of the Venus Nightside: The Thermal Structure and Water Abundance near the Surface, J. Geophys. Res., Vol. 101, 4595-4622, 1996.
10. Spurr, R.J.D., Kurosu, T.P., and Chance, K.V., A Linearized Discrete Ordinate Radiative Transfer Model for Atmospheric Remote Sensing Retrieval, J. Quant. Spectrosc. Radiat. Transfer, Vol. 68, 689-735, 2001.
11. Stamnes, K., Tsay, S.-C., Wiscombe, W., and Jayaweera, K., Numerically Stable Algorithm for Discrete Ordinate and Matrix Operator Method Radiative Transfer, Appl. Opt., 27, 2502-2509, 1988.
12. Rothman, L.S., Jacquemart, D., Barbe, A., Benner, D.C., Birk, M., Brown, L.R., Carleer, M.R. , Chackerian, C., Chance, K., Coudert, L.H., Dana, V., Devi, V.M., Flaud, J.M., Gamache, R.R., Goldman, A., Hartmann, J.M., Jucks, K.W., Maki, A.G., Mandin, J.Y., Massie, S.T., Orphal, J., Perrin, A., Rinsland, C.P., Smith, M.A.H., Tennyson, J., Tolchenov, R.N., Toth, R.A., Vander Auwera, J., Varanasi, P., Wagner, G., The HITRAN 2004 Molecular Spectroscopic Database. J. Quant. Spectrosc. Radiat. Transfer, Vol. 96, 139–204, 2005.
13. Karkoschka, E., Spectrophotometry of the Jovian Planets and Titan at 300- to 1000-nm Wavelength: The Methane Spectrum, Vol. 111, 174-192, 1994.
14. Hartmann, J.-M., Boulet, C., Brodbeck, C., van Thanh, N., Fouchet, T., Drossart, P., A Far Wing Lineshape for H_2 broadened CH_4 Infrared Transitions, J. Quant. Spectrosc. Radiat. Transfer, Vol. 72, 117-122, 2002.

15. Shardanand and Prasad Rao, A.D., Absolute Rayleigh Scattering Cross Sections of Gases and Freons of Stratospheric Interest in the Visible and Ultraviolet Regions, NASA Technical Note D-8442, 1-37, 1977.
16. Birnbaum, G., Borysow, A., and Orton, G.S., Collision-Induced Absorption of H_2-H_2 and H_2-He in the Rotational and Fundamental Bands for Planetary Applications, ICARUS, Vol. 12, 4-22, 1996.
17. Baines, K.H., and Hammel, H.B., Clouds, hazes, and the stratospheric methane abundance in Neptune, ICARUS, Vol. 109, 20-39, 1994.
18. Roe, H.G., Gavel, D., Max, C., de Pater, I. Gibbard, S., Macintosh, B., Baines, K.H., Near-Infrared Observations of Neptune's Tropospheric Cloud Layer with the Lick Observatory Adaptive Optics System, Vol. 122, 1636-1643, 2001.
19. Irwin, P.G.J., Sromovsky, L.A., Strong, E.K., Sihra, K., Teanby, N.A., Bowles, N., Calcutt, S.B., Remedios, J.J., Improved Near-Infrared Methane Band Models and k-Distribution Parameters from 2000 to 9500 cm^{-1} and Implications for Interpretation of Outer Planet Spectra, ICARUS, Vol. 181, 309-319, 2006.
20. Pryor, W.R., West, R.A., Simmons, K.E., and Delitsky, M., High-Phase-Angle Observations of Neptune at 2650 and 7500 Å: Haze Structure and Particle Properties, ICARUS, Vol. 99, 302-317, 1992.
21. Burgdorf, M., Orton, G.S., Davis, G.R., Sidher, S.D., Feuchtgruber, H., Griffin, M.J., and Swinyard, B.M., Neptune's Far-Infrared Spectrum from the ISO Long-Wavelength and Short-Wavelength Spectrometers, ICARUS, Vol. 164, 244-253, 2003.
22. Marten, A., D. Gautier, T. Owen, D.B. Saunders, H.E. Matthews, S.K. Atreya, R.P.J Tilanus, and Deane, J.R., 1993. First Observations of CO and HCN on Neptune and Uranus at Millimeter Wavelengths and the Implications for Atmospheric Chemistry. Ap. J., Vol. 406, 285-297, 1993.
23. Hesman, B.E., Davis, G.R., Matthews, H.E., Orton, G.S., The Abundance Profile of CO in Neptune's Atmosphere, ICARUS, Vol. 186, 342-353, 2007.
24. Orton, G.S., Aitken, D.K., Smith, C., Roche, P.F., Caldwell, J., Snyder, R., The Spectrum of Uranus and Neptune at 8-14 and 17-23 Microns, ICARUS, Vol. 70, 1-12, 1987.
25. Orton, G.S., Baines, K.H., Caldwell, J., Romani, P., Tokunaga, A.T., West, R.A., Calibration of the 7- to 14-Micron Brightness Spectra of Uranus and Neptune, ICARUS, Vol. 85, 257-265, 1990.
26. Hammel, H.B., Lynch, D.K., Russell, R.W., Sitko, M.L., Bernstein, L.S., and Hewagama, T., Mid-Infrared Ethane Emission on Neptune and Uranus, Ap. J.. Vol. 644, 1326-1333, 2006.
27. Hammel, H.B. personal communications, 2006.
28. Orton, G.S., Lacy, J.H., Achtermann, J.M., Parmar, P. and Blass, W.E., Thermal Spectroscopy of Neptune: The Stratospheric Temperature, Hydrocarbon Abundances, and Isotopic Ratios, ICARUS, Vol. 100, 541-555, 1992.
29. Fink, U. and Larson, H.P., The Infrared Spectra of Uranus, Neptune, and Titan from 0.8 to 2.5 Microns, Ap. J., Vol. 233, 1021-1040, 1979.